Available online at www.sciencedirect.com
SCIENCE DIRECT®
Journal of Nuclear Materials 337–339 (2005) 520–524
journal of nuclear materials
www.elsevier.com/locate/jnucmat

Neutral pressure behavior for diverted discharges in the Wendelstein 7-AS Stellarator

K. McCormick *, P. Grigull, R. Burhenn, H. Ehmler, Y. Feng, L. Giannone, G. Haas, F. Sardei, The NBI-, ECRH- and W7-AS Teams

Max-Planck-Institut für Plasmaphysik, EURATOM, Boltzmannstrasse 2, 85748 Garching, Germany

Abstract

On the W7-AS stellarator, the subdivertor neutral pressure in an up–down divertor pair as well as at two points in the vicinity of a lower divertor module in the main chamber are measured. Results are presented for $\iota_a = 5/9$ island divertor discharges under conditions of normal confinement (NC) and the HDH-mode for: $\bar{n}_e \sim 0.1$–4×10^{20} m^{-3}, $P_{ecrh} = 0.5$–1.5 MW, $P_{nbi} = 2$ MW, and H^+ and D^+ plasmas, with both normal- and reversed-B_t for H^+. Subdivertor pressures are in the range 1–2×10^{-3} mbar for HDH conditions. For plasma detachment at the target plates a strong up–down pressure asymmetry arises, with $p_{up}/p_{down} \leqslant 5$. The asymmetry reverses with reversed B_t. Main vessel pressures are a factor of 5–10 lower than the average subdivertor pressure for H^+, with D^+ plasmas exhibiting still lower values.

PACS: 52.55.c
Keywords: W7AS; Edge plasma; Cross-field transport; Divertor; Divertor neutrals

1. Introduction

In its last operational phase the Wendelstein 7-AS Stellarator ($R = 2$ m, $a \sim 12$ cm for $\iota_a \sim 5/9$) was equipped with divertor modules allowing a first-time experimental evaluation of the concept of a boundary-island divertor. Intensive divertor experiments were carried out over the period April 2001 until July 2002, when W7-AS operation was terminated. This paper reports on neutral pressure measurements in the subdivertors and in the main chamber, in order to document conditions on W7-AS for various operational scenarios and to establish a database for future edge code validation.

For these investigations the plasma is bounded by a separatrix formed from naturally-occurring magnetic islands, at an edge iota value $\iota_a = 5/9$ (Fig. 1). The five top-bottom discrete divertor module pairs (one pair for each period, covering ~27% of the circumference) provide a carbon plasma-target interaction region. The walls are of stainless steel.

Four ASDEX-type gauges [1] were placed in subdivertors (3 upper and one lower). Five were situated in the main chamber, all within one period to monitor the 3D pressure variations expected to accrue. Since no significant periodic toridal variations were registered, results are reported from only one up–down divertor pair, p_{up}

* Corresponding author. Tel.: +49 89 3299 1932; fax: +49 89 3299 2584.
E-mail address: gkm@ipp.mpg.de (K. McCormick).

0022-3115/$ - see front matter © 2004 Published by Elsevier B.V.
doi:10.1016/j.jnucmat.2004.10.052

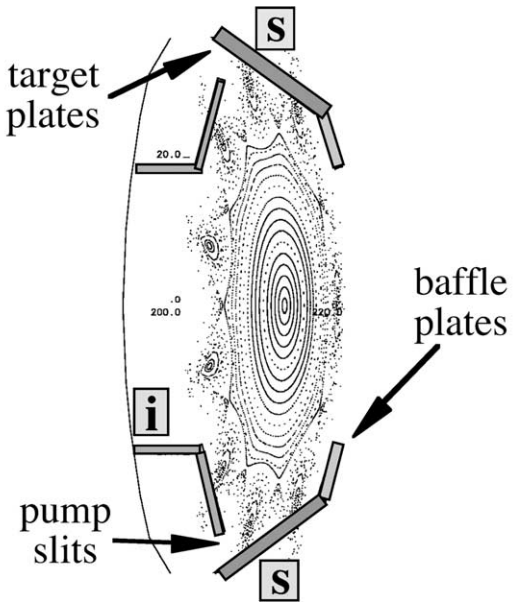

Fig. 1. Flux surface plot for the standard divertor configuration at $\iota_a = 5/9$. The positions of the pressure gauges in the subdivertors (S) and main chamber at the inner vessel wall (i) are symbolically indicated. Distance from nearest x-point to target plates ~39 mm.

and p_{down} (positions indicated in Fig. 1). In the main chamber, the pressures seen by a gauge at the inner wall p_{in} (Fig. 1) as well as a gauge p_{end} (at the end of the same lower divertor at the bottom of the torus) are discussed. Actually, such gauges register the local gas flux, and not pressure. However, due to baffling the neutrals essentially attain room temperature in the detector head, and thus the pressures quoted represent room-temperature equivalents.

Measurements are reported for two heating schemes: ECRH for $\bar{n}_{\mathrm{e}}$ extending to near cutoff, and NBI for $\bar{n}_{\mathrm{e}}$ up to $4 \times 10^{20}\,\mathrm{m}^{-3}$. With the standard $\iota_a = 5/9$ configuration an entirely new stellarator plasma confinement regime was discovered shortly after beginning high-power NBI, high-density divertor operation: the high-density H-mode (HDH) [2–6]. HDH is an ELM-free, stationary H-mode exhibiting high separatrix densities n_{es} and plasma radiation $P_{\mathrm{rad}}(r)$ concentrated at the edge. Below the threshold density $\bar{n}_{\mathrm{e}}^{\mathrm{th}}$ for entering HDH, normal confinement (NC) exists, where the enhanced particle confinement associated with higher line-averaged density $\bar{n}_{\mathrm{e}}$ for a stellarator plasma leads to non-stationary conditions and eventual radiation collapse if $\bar{n}_{\mathrm{e}}$ is too high [7,8]. Since $\bar{n}_{\mathrm{e}}^{\mathrm{th}}$ is beyond the cutoff density of $1.2 \times 10^{20}\,\mathrm{m}^{-3}$ for 2nd harmonic ECRH at 140 GHz, only NC conditions are accessible with ECRH. A series of density scans over $\bar{n}_{\mathrm{e}} \sim 1\text{–}11 \times 10^{19}\ \mathrm{m}^{-3}$ for $P_{\mathrm{ecrh}} = 0.5$, 1 and 1.5 MW are studied in Section 2.1. Here the emphasis is on the parametric behavior of subdivertor pressures. Section 2.2 considers $P_{\mathrm{nbi}} = 2$ MW (P_{abs} = absorbed power ~ 1.4 MW) heating over $\bar{n}_{\mathrm{e}} \sim 0.7\text{–}4 \times 10^{20}\ \mathrm{m}^{-3}$ for $H^0 \rightarrow H^+$ and $D^0 \rightarrow D^+$ plasmas, covering both NC- and HDH-regimes. Further, H^+ plasmas with reversed toroidal field B_{t} are examined to document that systematic p_{up}–p_{down} asymmetries with $\bar{n}_{\mathrm{e}}$ and P_{rad} invert with the field direction.

2. Experiments

2.1. Normal confinement discharges with ECRH heating

The behavior of edge/divertor parameters vs. density are studied in three density ramp discharges, each at a different power level $P_{\mathrm{ecrh}} = 0.5$, 1 and 1.5 MW. The density ramp takes place over 0.1–0.8 s. Investigations under the same conditions with steady-state discharges, but at lower densities, show little difference to the dynamic situation of a ramp [5]. The behavior of the lower divertor pressure p_{down} (p_{up} is the same) is given as a function of $\bar{n}_{\mathrm{e}}$ for the three power levels (top, Fig. 2). All three curves exhibit a saturation with increasing $\bar{n}_{\mathrm{e}}$. The augmentation of pressure with P_{ecrh} is obvious. Since p_{down} is expected to be a direct function of the separatrix density n_{es}, (values from Li-beam) and only indirectly $\bar{n}_{\mathrm{e}}$, the same data is given vs. n_{es} (middle graph, Fig. 2): A universal curve appears to describe all power levels at the lower end of each n_{es} range. At higher n_{es} these separate and finally saturate as well. It is evident that n_{es} is itself a function of power, with n_{es} increasing with power for a given $\bar{n}_{\mathrm{e}}$. In any case, in this low-n_{e} regime where plasma plugging of the pump slit to the subdivertor region should not be important, one expects p_{down} to be directly related to the particle flux to the target plate. This is explored in the lower graph of Fig. 2, where p_{down} is given vs. the ion saturation current I_{sat} to a Langmuir probe situated near the separatrix strike zone in the lower divertor. Here, the data is unified. The scatter in the I_{sat} coordinate is due to the appearance of ELM activity at higher densities, which is not resolved by the pressure gauges.

Initial simulation calculations with the edge code EMC3/EIRENE [9] have been carried out to address the observed pressure behavior as a function of n_{es} and P_{ecrh}. Assumption of a perpendicular diffusion coefficient varying as $D \sim P_{\mathrm{ecrh}}$ describes the power dependence rather well. Further, if $D \sim 1/n_{\mathrm{es}}$ is taken, the offset-linear behavior at higher $\bar{n}_{\mathrm{e}}$ can be characterized.

2.2. NBI discharges, NC and HDH regimes

Fig. 3 shows the behavior vs. $\bar{n}_{\mathrm{e}}$ for three different datasets – of the energy confinement time τ_{E} and the

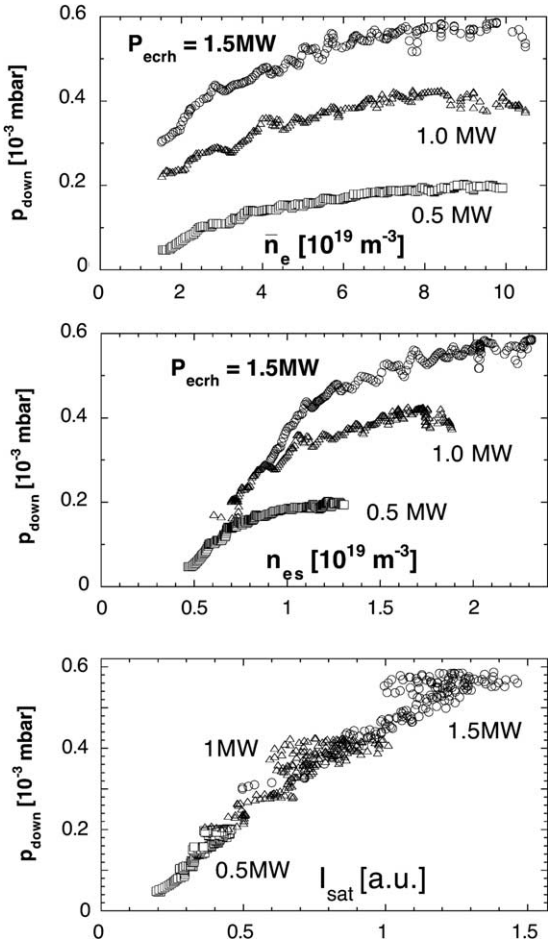

Fig. 2. Subdivertor neutral pressure for three density-ramp discharges at powers of $P_{ecrh} = 0.5$, 1 and 1.5 MW. #51294,95,97. Top: vs. line-averaged density $\bar{n}_e$; Middle: vs. n_{es}; Bottom: vs. I_{sat} to a target plate Langmuir probe. $B_t = -2.5$ T, $\iota_a = 5/9$.

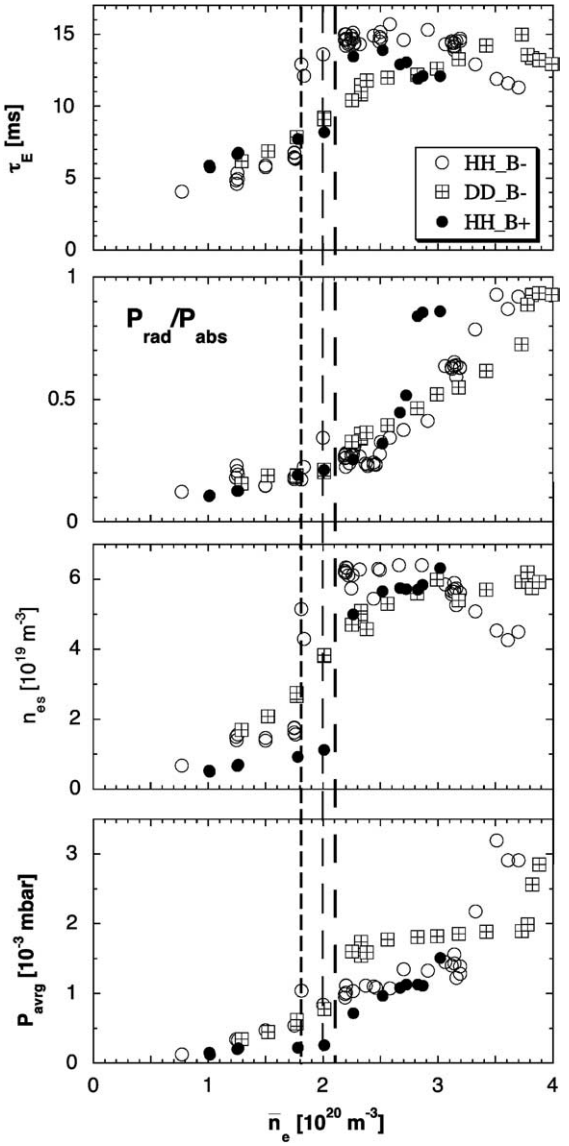

Fig. 3. Energy confinement time τ_E, P_{rad}/P_{abs}, n_{es} and $p_{avrg} = (p_{up}+p_{down})/2$ for three stationary discharge series: $H^0 \rightarrow H^+$ ($B_t = \pm 2.5$ T) and $D^0 \rightarrow D^+$ ($B_t = -2.5$ T). $P_{nbi} = 2$ MW. $\bar{n}_e^{th}$ is indicated (from left to right) for H^+ (-2.5 T), D^+ (-2.5 T) and H^+ ($+2.5$ T).

parameters expected to have an impact on subdivertor pressure: the normalized total plasma radiation P_{rad}/P_{abs} and n_{es}. The average divertor pressure $p_{avrg} = (p_{up} + p_{down})/2$ is used since there are systematic differences between p_{up} and p_{down} (discussed below). All discharges are quasi-stationary. Data from both H^+ and D^+ plasmas are presented as it is known from previous work that the n_e- and T_e-profiles for D^+ are different [4], which can be expected to influence neutral pressures. A reverse-B_t series in H^+ is included, first in order to investigate the nature of HDH for counter-NBI and secondly to check if the pronounced p_{up}–p_{down} asymmetries seen for the normal field direction also correspondingly reverse.

The NC→ HDH transition densities $\bar{n}_e^{th}$ differ in all three cases: H^+ $(-2.5\,\mathrm{T}) \sim 1.8 \times 10^{20}\,\mathrm{m}^{-3}$, D^+ $(-2.5\,\mathrm{T}) \sim 2 \times 10^{20}\,\mathrm{m}^{-3}$ and H^+ $(+2.5\,\mathrm{T}) \sim 2.1 \times 10^{20}\,\mathrm{m}^{-3}$. The step in τ_E is evident for H^+. For D^+, because the n_e- and T_e-profiles evolve differently with $\bar{n}_e$ [4], there is no marked spontaneous improvement in τ_E. However, the impurity lifetime, as determined by the spatio-temporal behavior of laser-ablated aluminum [3,4,7], drops dramatically at the transition (not shown), a primordial indicator of HDH. Plasma detachment at the target plate is present for those cases where τ_E decreases with increasing $\bar{n}_e$. The detachment boundaries are: H^+ $(-2.5\,\mathrm{T}) \sim 3 \times 10^{20}\,\mathrm{m}^{-3}$, D^+

$(-2.5\,\mathrm{T}) \sim 3.7\times10^{20}\,\mathrm{m}^{-3}$ and H^+ $(+2.5\,\mathrm{T}) \sim 2.5\times10^{20}\,\mathrm{m}^{-3}$. For H^+ ($\pm2.5\,\mathrm{T}$) detachment occurs when $P_{rad}/P_{abs} > 50\%$. D^+ is able to sustain a considerably higher level of radiation before detaching (although in all cases the highest P_{rad} level is about 90%). This behavior is related to the fact that $D^0 \rightarrow D^+$ heating takes place much closer to the edge, thereby leading to broader n_e- and T_e-profiles [4].

Both cases of H^+ ($\pm2.5\,\mathrm{T}$) show a sharp increase in n_{es} at the NC $\rightarrow$ HDH transition, whereas no jump is evident for D^+. The behavior of p_{avrg} in the NC regime is linear with n_{es}, with most points for H^+ and D^+ lying on a curve given by p_{avrg} $(10^{-3}\,\mathrm{mbar}) = 0.05 + 0.19 n_{es}$ $(10^{19}\,\mathrm{m}^{-3})$ (not shown). In fact, for H^+ almost all points lie within ±20% of the curve $p_{avrg} = 0.23 n_{es}$ regardless of regime. The case of D^+ is particularly interesting at $\bar{n}_e^{th}$ where p_{avrg} increases more than a factor of two whereas the change in n_{es} is only ~25%. Before detachment p_{avrg} (D^+) is clearly higher than that for H^+. Both are in the range $1\text{–}2\times10^{-3}$ mbar. A prominent feature of H^+ and D^+ for the normal field cases is a dramatic increase in p_{avrg} at detachment, rising up to 3×10^{-3} mbar. This is associated with the appearance of a strong p_{up}–p_{down} asymmetry at detachment (Fig. 4): For normal field, p_{down} decreases slightly at detachment and then remains constant whereby p_{up} continually increases as the plasma is driven further into detachment. The asymmetry is inverted with reversed field as seen in the top and bottom plots of Fig. 4 where p_{down}/p_{up} is taken for the H^+ (+2.5 T) case and found to behave rather the same as p_{up}/p_{down} for H^+–D^+ (−2.5 T). The only difference is the onset point of detachment. Note that the pressure ratios change uniformly over the entire $\bar{n}_e$-range until detachment. The D^+ data (middle, Fig. 4), which was taken in one series and has the greatest extent in $\bar{n}_e$ over the attached regime, shows the systematic variations in p_{up} and p_{down} with $\bar{n}_e$. The cohesiveness of all data is more clearly illustrated when plotted vs. P_{rad}/P_{abs} (bottom, Fig. 4), where the points for D^+ and counter-NBI H^+ now overlap.

The onset of the p_{up}–p_{down} asymmetry is always accompanied by an asymmetry in the poloidal P_{rad} distribution, with the appearance of an enhanced radiation zone at the inside near the upper divertor. Investigation of H_α/H_γ radiation over the target plates points to the formation of a recombining region at the upper divertor for normal field polarity [10]. Thus, it would appear that some unknown effect causes a recombination zone in the upper divertor to originate at detachment, thereby effecting a higher neutral production which is registered principally in the upper subdivertor chamber. Since the recombination is correlated with the asymmetric increase in P_{rad}, it not surprising that P_{rad}/P_{abs} serves as a good ordering parameter.

With respect to main-chamber neutral pressures, p_{end}/p_{avrg} always remains below 10% and is lower for

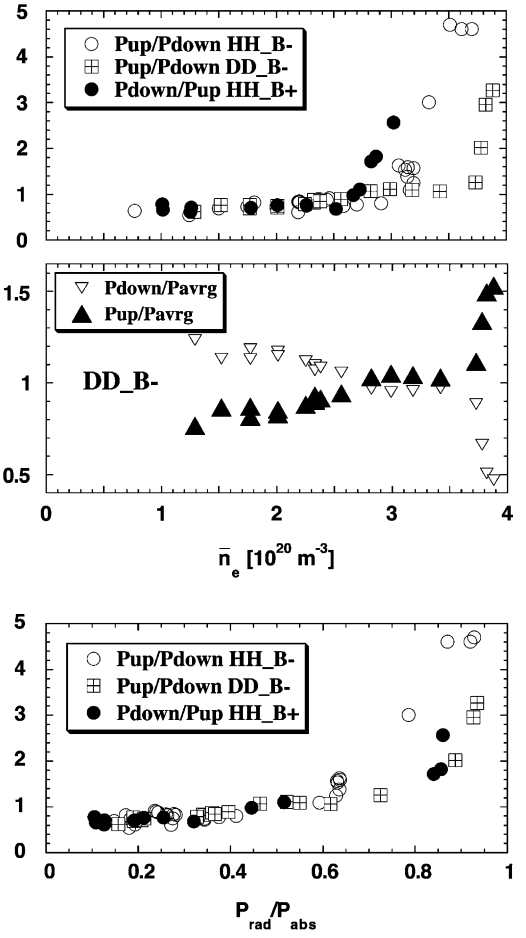

Fig. 4. Pressure ratio p_{up}/p_{down} ($B_t = -2.5\,\mathrm{T}$) or p_{down}/p_{up} ($B_t = +2.5\,\mathrm{T}$) for the discharges of Fig. 3 vs. $\bar{n}_e$ (top) or P_{rad}/P_{abs} (bottom).

D^+, being about 6% at most. For H^+ below detachment ($p_{avrg} < 1.6\times10^{-3}$ mbar) the ratio augments with increasing p_{avrg}, changing from ~5% to 10% over the range. Pressures near the inner lip of the lower divertor p_{in} also increase with p_{avrg}, varying over p_{in}/p_{avrg} ~5–20%. D^+ discharges take on values ~3–12%.

3. Discussion and summary

In the low-density NC-regime a strong dependence of subdivertor pressure p_{down} ($= p_{up}$) is found on P_{ecrh}. Furthermore, p_{down} increases with n_{es} in an offset-linear fashion, showing signs of saturation at higher n_{es}. Preliminary EMC3/EIRENE calculations indicate that these observations can be simulated by scaling the perpendicular diffusion coefficient in the SOL as $D \sim P_{sol}/n_{es}$, but further studies are necessary. For NBI-heating there is no evident saturation effect of p_{avrg} with n_{es} over the

entire range. Rather, $p_{avrg}(10^{-3}\,mbar) \sim 0.23 \pm 20\%$ $n_{es}(10^{19}\,m^{-3})$ accounts for almost all H^+ values. On the other hand, the increase in p_{avrg} at the NC → HDH transition for D^+ is over-proportional to the change in n_{es}. This may reflect a fundamental increase in particle transport at the plasma edge leading to an augmentation of subdivertor pressure.

Comparing the $P_{nbi} = 2\,MW$ discharges for H^+ ($\pm 2.5\,T$) in the NC-regime to the $P_{ecrh} = 1.5\,MW$ results we find that p_{avrg} is very similar to p_{down} for ECRH for a given n_{es}. But, it is not apparent from the data of Fig. 3 that p_{avrg} is beginning to saturate at the $\bar{n}_e$ values preceding the NC → HDH transition. For attached HDH cases, p_{avrg} for H^+ is $\sim 1.2 \times 10^{-3}$ mbar, whereas for D^+ p_{avrg} is $\sim 1.8 \times 10^{-3}$ mbar. These values are in excess of those needed to pump the neutrals (via Ti-gettering) fueled through NBI ($\sim 2.5 \times 10^{20}$ s^{-1} at $P_{nbi} = 2\,MW$), i.e. to maintain steady-state density control. In fact, for HDH discharges the passive pumping of the graphite target plates is adequate to achieve steady-state, with He glow-discharge cleaning necessary only at the beginning of the day. At detachment large subdivertor pressures accrue, rapidly increasing with deeper penetration into detachment, finally producing average pressures greater than 3×10^{-3} mbar. An interesting aspect is that detachment goes hand-in-hand with a strong up–down asymmetry in subdivertor pressure: For the normal field direction, p_{down} drops marginally and then remains constant as detachment progresses, while p_{up} increases dramatically up to values approaching 5×10^{-3} mbar. The pressure increase is correlated with the appearance of a localized recombination region in the upper divertor. It is thought this is at least one source of increased neutral production. Corresponding simulations with EMC3/EIRENE are not possible since recombination has not yet been implemented. In any case, an asymmetry is not expected – possibly indicating the influence of unidentified ($E \times B$?) drifts in the SOL. This view is supported by the observation that the up–down asymmetry reverses when the B_t direction is reversed. In terms of plasma operation, this asymmetry has little influence on up–down power deposition and is not readily observable except in the subdivertor pressure. It is interesting to note that if recombination is a principal additional source of neutrals in the upper divertor (for 2.5 T) on W7-AS, then similar in–out pressure asymmetries might be expected on tokamaks, where the inner divertor is often driven to volume recombination. This is not observed, either because the in–out pressures are not measured or communication between the inside and outside of the subdivertor regions is too good to permit an obvious asymmetry to develop.

With respect to main chamber pressures, the gauge at the end of the lower divertor registers $p_{in}/p_{avrg} \sim 5$–10%, increasing with $\bar{n}_e$ for H^+ and ~3–6% for D^+. At the inner wall just above the lower divertor p_{in} ~5–20%, also increasing with $\bar{n}_e$, whereas D^+ shows ratios ~3–12%. Absolutely, the main chamber pressures in the HDH regime (before detachment) are ~ 1–2×10^{-4} mbar. At detachment these can increase to beyond 3×10^{-4} mbar. Attainment of H-mode conditions on W7-AS is not impaired by such high pressures. Indeed, until the nature of the HDH-mode is more clearly understood, it cannot be ruled out that these are a corollary of HDH confinement. Finally, although not discussed here, a limiter HDH-mode has been found to yield similar subdivertor and main chamber pressures as diverted discharges.

References

[1] G. Haas, H.-S. Bosch, Vacuum 51 (1998) 39.
[2] P. Grigull et al., Plasma Phys. Control. Fusion 43 (2001) A175.
[3] K. McCormick et al., Phys. Rev. Lett. 89 (2002) 015001.
[4] K. McCormick et al., J. Nucl. Mater. 313–316 (2003) 1131.
[5] K. McCormick et al., Europhys. Conf. Abst. 25A (2001) 2097.
[6] K. McCormick et al., in: Proceedings of 14th International Workshop on Stellarators, Greifswald, 2003.
[7] R. Burhenn et al., Fusion Sci. Technol. 46 (2004) 115.
[8] L. Giannone et al., Plasma Phys. Control. Fusion 42 (2000) 603.
[9] Y. Feng, F. Sardei, et al., Contrib. Plasma Phys. 44 (1–3) (2004) 57.
[10] U. Wenzel et al., J. Nucl. Mater. 313–316 (2003) 1098.